Chapter 3

Complex Periodic Behaviour in a Neural Network Model with Activity-Dependent Neurite Outgrowth

A. van Ooyen & J. van Pelt, J. Theor. Biol., in press.

In the previous chapter we studied networks in which all the cells reacted in the same way on electrical activity. Since experiments have shown that neurons may in fact react differentially, we study in this chapter networks made up of cells among which the level of activity above which the neurites of a cell retract varies. We show that this can lead to complex periodic behaviour in electrical activity (and connectivity) of individual cells. The precise behaviour depends on the spatial distribution of the cells and the distribution of the outgrowth properties over the cells. Any other cellular property that adapts slowly to electrical activity such that neuronal activity is attempted to be maintained at a given level, can lead to similar results.

3.1 Introduction

Electrical activity plays an important role in the development of neurons into functional networks. Many processes that determine connectivity and neuronal function are modulated by electrical activity (see Chapter 1). As a result of these activity-dependent processes, a reciprocal influence exists between neuronal activity ('fast dynamics') and the development of connectivity and neuronal function ('slow dynamics'). In this article we focus on activity-dependent neurite outgrowth.

A number of studies have demonstrated that neurotransmitters and electrical activity can directly affect neurite outgrowth (for review see Mattson, 1988). Neurites stop growing or even retract under conditions of (high) neuronal activity (Cohan & Kater, 1986; Fields *et al.*, 1990a; Schilling *et al.*, 1991; Grumbacher-Reinert & Nicholls, 1992). Such alterations in outgrowth are mediated by changes in intracellular calcium concentrations ($[Ca^{2+}]_{in}$) (Cohan *et al.*, 1987; Kater *et al.*, 1988; Mattson, 1988; Kater & Mills, 1991). Depolarization leads to increases in $[Ca^{2+}]_{in}$, and many aspects of the motility of neurites are regulated by Ca^{2+}. In connection with these observations, the Ca^{2+} theory of neurite outgrowth has been proposed (e.g., Kater *et al.*, 1988; 1990), which states that low $[Ca^{2+}]_{in}$ (low level of electrical activity) stimulates outgrowth, higher concentrations cause a cessation of outgrowth, and still higher concentrations (high level of electrical activity) lead to regression of neurites. In addition, outgrowth is also blocked if $[Ca^{2+}]_{in}$ is too low.

Previously we studied networks in which the critical level of electrical activity (or $[Ca^{2+}]_{in}$) above which the neurites of a cell retract, is the same for all cells. However, this level is in fact different for different classes of neurons (Guthrie *et al.*, 1988; Kater *et al.*, 1988; 1990). What constitutes a high level of electrical activity for one neuron may actually fall within the permissive outgrowth range of another. Such differences could be due to different initial or basal levels of intracellular Ca^{2+} or to different Ca^{2+} buffering capacities (Kater *et al.*, 1988). In the light of this, we consider in the present study networks made up of cells that have such differences in outgrowth properties.

The model is described in Section 3.2. A brief summary of previous results is given in Section 3.3.1. The periodic behaviour with respect to connectivity and electrical activity in cells within a (large) network is described in Section 3.3.2. This behaviour will be qualitatively explained in Section 3.3.3 using a series of simplified models. In Section 3.3.4 it is shown that the same results are obtained when neurite outgrowth is replaced by any other slow, activity-dependent process that act to stabilize neuronal electrical activity levels ('homeostasis'). Preliminary results of this study have been reported in Van Ooyen & Van Pelt, 1994b.

3.2 The Model

The model is used as a tool to explore the possible consequences of activity-dependent neurite outgrowth for network behaviour, in a general and qualitative sense. The initially disconnected neurons organize themselves into a network under influence of endogenous electrical activity only. Growing neurons are modelled as expanding neuritic fields, and the outgrowth of each neuron depends upon its own level of activity. Neurons become connected when their neuritic fields overlap. In this study, all connections are taken to be excitatory. The model is inspired in part by tissue cultures of dissociated cerebral cortex cells (Van Huizen, 1986; Van Huizen *et al.*, 1985, 1987a; Ramakers *et al.*, 1991), which become organized into a network by neurite outgrowth and synaptogenesis without the influence of external input.

The model is the same as the one used in previous studies (Van Ooyen & Van Pelt, 1994a, b; Van Ooyen *et al.*, 1995), and is studied both analytically and by means of numerical solution, employing the variable time step Runge-Kutta integrator provided by Press *et al.* (1988). The simplified models (Sections 3.3.3 and 3.3.4) are analysed using GRIND (De Boer, 1983).

3.2.1 Neuron Model

To describe neuronal activity, the shunting model (Grossberg, 1988) is used, in which excitatory inputs drive the membrane potential towards a finite maximum or saturation potential. For a purely excitatory network, after transformation to dimensionless equations (e.g., Carpenter, 1983; Van Ooyen *et al.*, 1995a), this model becomes

$$\frac{dX_i}{dT} = -X_i + (1 - X_i) \sum_{j=1}^{N} W_{ij} F(X_j), \tag{3.1}$$

where X_i represents the (time averaged) membrane potential of cell i, scaled between the saturation potential (set to 1) and the resting membrane potential (set to 0), N is the total number of excitatory cells, T is the time in units of the membrane time constant, W_{ij} is the connection strength between neuron j and i ($W_{ij} \geq 0$; W_{ij} is defined in Section 3.2.2), and

$$F(X) = \frac{1}{1 + e^{(\theta - X)/\alpha}}, \tag{3.2}$$

where $F(X)$ is the mean firing rate (with its maximum set to 1), α determines the steepness of the function and θ represents the firing threshold. The low firing rate when the membrane potential is sub-threshold can be considered as representing spontaneous activity, arising from threshold or membrane potential fluctuations (for references see Van Ooyen *et al.*, 1995a).

3.2.2 Outgrowth and Connectivity

Neurons are randomly placed on a two-dimensional surface. Each neuron is given a circular 'neuritic field', the radius of which is variable. When two such fields overlap, both neurons become connected with a strength proportional to the area of overlap:

$$W_{ij} \equiv A_{ij} S, \tag{3.3}$$

where $A_{ij} = A_{ji}$ is the amount of overlap ($A_{ii} = 0$), representing the total number of synapses formed reciprocally between neurons i and j, while S represents the average synaptic strength. In this abstraction, no distinction has been made between axons and dendrites, but in Section 3.3.4 it is tested whether or not such asymmetry affects the results.

Since the effect of activity on outgrowth is mediated by intracellular calcium, and since the firing of action potentials leads to increases in $[Ca^{2+}]_{in}$ (see Section 3.1), we take the outgrowth of each individual cell to be dependent upon its firing rate:

$$\frac{dR_i}{dT} = \rho G(F(X_i)), \tag{3.4}$$

where R_i is the radius of the circular neuritic field of neuron i, and ρ determines the rate of outgrowth. Note, that connection strength is not directly modelled but is a function of neuritic field size. The function G has a zero crossing at $u = \epsilon_i$ such that

$$\begin{cases} for\ u < \epsilon_i & G(u) > 0 \\ for\ u > \epsilon_i & G(u) < 0 \\ for\ u = \epsilon_i & G(u) = 0. \end{cases} \tag{3.5}$$

Equation 3.5 is a phenomenological description of the theory of Kater *et al.* (see Section 3.1) to the effect that relatively low electrical activity (i.e., below 'setpoint' ϵ_i) allows neurite outgrowth, while sufficiently high activity (i.e., above ϵ_i) causes neurites to retract (excluding that outgrowth also does not seem to take place at very low levels of activity). To take into account the empirical observation that the level of electrical activity (or $[Ca^{2+}]_{in}$) above which the neurites of a cell retract is not the same for all cells (see Section 3.1), ϵ_i is allowed to differ among cells.

For the network model (Sections 3.3.1 and 3.3.2), the following growth function was used:

$$G(F(X_i)) = 1 - \frac{2}{1 + e^{(\epsilon_i - F(X_i))/\beta}}, \tag{3.6}$$

where β determines the steepness of G. This function remains in the bounded range $< -1, 1 >$.

Outgrowth of neurons is on a time scale of days or weeks (e.g., Van Huizen *et al.*, 1985, 1987a; Van Huizen, 1986; Schilling *et al.*, 1991), so that connectivity is quasi-stationary on the time scale of membrane potential dynamics (i.e., ρ small). To avoid unnecessarily slowing down the simulations, ρ is chosen as large as possible while maintaining the quasi-stationary approximation. In the simulations of the network model, we use $\rho = 0.0001$. As nominal values for the other parameters, for both the network model and the simplified models, we chose $\theta = 0.5$, $\alpha = 0.10$, $\beta = 0.10$. For ϵ, all possible values are considered.

3.3 Results

3.3.1 Identical Outgrowth Function

In this section we briefly summarize the previous results relevant for this study. The variations in $\mathbf{W}$ take place much more slowly than those in X, so that $\mathbf{W}$ can in a first approximation be considered as a parameter of the system. For a given $\mathbf{W}$ in a purely excitatory network, the equilibrium points are solutions of [see Eq. (3.1)]

$$0 = -X_i + (1 - X_i) \sum_{j=1}^{N} W_{ij} F(X_j) \qquad \forall i. \tag{3.7}$$

If all the cells have the same ϵ_i, and the variations in X_i are small (relative to $\bar{X}$, the average membrane potential of the network), the average connection strength $\bar{W}$ can be written as a function of $\bar{X}$ (Van Ooyen & Van Pelt, 1994a):

$$\bar{W} = \frac{\bar{X}}{(1 - \bar{X})F(\bar{X})} \qquad 0 \leq \bar{X} < 1. \tag{3.8}$$

The slow movement of the system determined by the dynamics in connectivity takes place along the manifold defined by Eq. 3.8 [see Fig. 3.1(a)]. It is the so-called slow manifold, and is the same as the equilibrium manifold of $\bar{X}$ (defined by $d\bar{X}/dT = 0$) for $\bar{W}$ as a parameter of the system. The manifold is S-shaped ('hysteresis loop') which underlies the emergence of overshoot and oscillations (further see caption of Fig. 3.1).

3.3.2 Network of Cells Having Different Outgrowth Functions

For a network in which ϵ is different for different cells, the resulting network behaviour depends also on the spatial distribution of the cells (e.g., random as opposed to regular) as well as on the distribution of the ϵ values over the cells. Especially if the spatial distribution of cells is such that all of them become strongly connected to many of their neighbours (as will happen with a regular distribution of cells), not all of the cells need to have an ϵ in

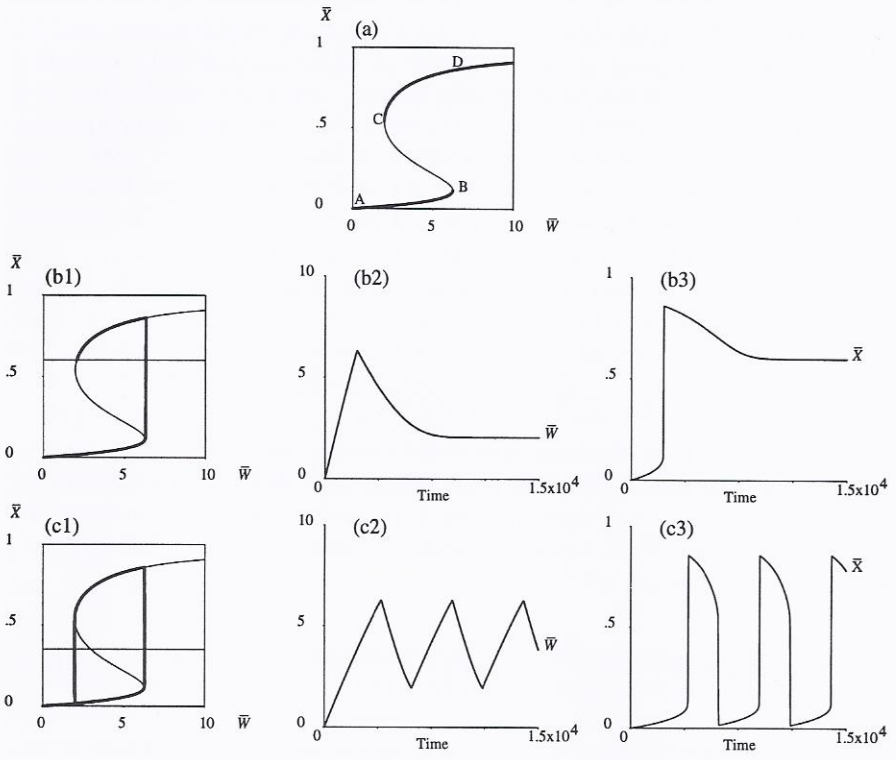

Fig. 3.1 Hysteresis. **(a)** The S-shaped slow manifold of $\bar{X}$ ($d\bar{X}/dT = 0$) in the $(\bar{W}, \bar{X})$-plane ($\bar{W} = (1/N)\sum_{i=1,j=1}^{N} W_{ij}$), as defined by Eq. (3.8). When $\bar{W}$ is regarded as a parameter, states on BC are unstable, while the others are stable (bold lines). The horizontal line indicate $\bar{X} = F^{-1}(\epsilon)$ (F^{-1} is the inverse of F). Above and below that line, $\bar{W}$ decreases and increases, respectively [see Eq. (3.6)]. The connectivity, $\bar{W}$, is quasi-stationary on the time scale of membrane potential dynamics, and, starting at A, $\bar{X}$ will follow the branch AB, until it reaches B, where it jumps to the upper branch. **(b1)** If the intersection point of the horizontal line is on CD, $\bar{W}$ decreases again, and a developing network has to go through a phase in which $\bar{W}$ is higher than in the final situation (i.e., 'overshoot' in $\bar{W}$). The trajectory is shown as a bold line. In **(b2)** $\bar{W}$, and in **(b3)** $\bar{X}$ is shown against time. **(c1)-(c3)** An ϵ such that the intersection point is on BC, results in regular oscillations.

the non-oscillatory range (see Fig. 3.1) in order for both the network as a whole and the individual cells to show an absence of oscillations (in both connectivity and electrical activity). For example, in a network consisting of 16 regularly placed cells, in which only 5 cells have $\epsilon = 0.8$ (which, if all cells had this value, would cause an overshoot in connectivity and no subsequent oscillations), and the rest have $\epsilon = 0.4$ (which, if all cells had this value, would

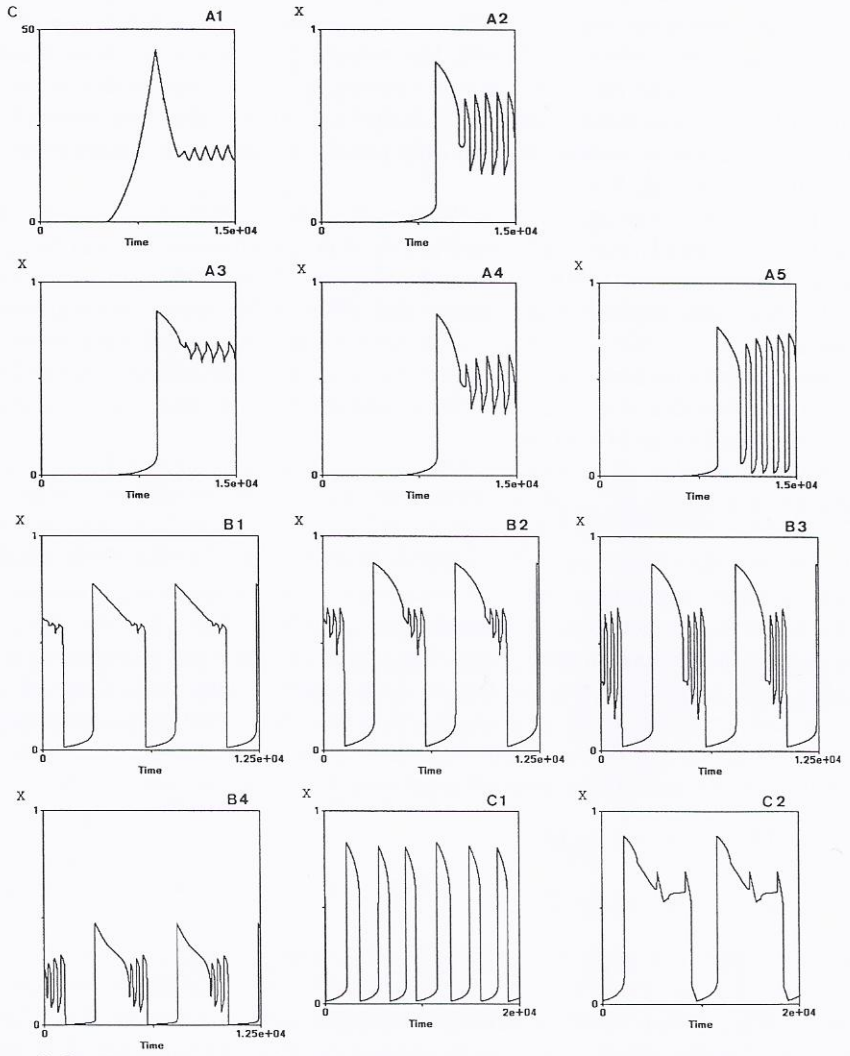

Fig. 3.2 Behaviour of individual cells in a network [governed by Eqs (3.1) and (3.6)]. **(a)** Network of 16 cells placed on a grid. Five cells have $\epsilon = 0.8$, the rest has $\epsilon = 0.4$. **(a1)** Overshoot in total connectivity ($C = \sum_{i=1,j=1}^{N} A_{ij}$). **(a2)** Average membrane potential in the network. **(a3)-(a5)** Membrane potential of 3 different cells. The cell of (a4) has $\epsilon = 0.4$, the rest has $\epsilon = 0.8$. **(b)** Membrane potential of 4 different cells in a network of 16 randomly placed cells in which ϵ is uniformly distributed between 0.05 and 0.8. In all figures the initial transients are skipped. **(b1)** $\epsilon = 0.65$. **(b2)** $\epsilon = 0.67$. **(b3)** $\epsilon = 0.36$. **(b4)** $\epsilon = 0.10$. **(c)** Network consisting of a group of 2 cells (both have $\epsilon = 0.68$) neighbouring to a large group of 19 cells (all have $\epsilon = 0.15$). Initial transients are skipped. **(c1)** $\epsilon = 0.15$. **(c2)** $\epsilon = 0.68$.

cause sustained oscillations in connectivity and electrical activity) still shows a 'normal' overshoot sequence, without any oscillations (also not in any of the individual cells). With a different, less central distribution of these 5 cells, the individual cells show oscillations between quiescent and activated state with different amplitudes [see Fig. 3.2(a3)-(a5)]. Note, that the network as a whole still shows overshoot with only small oscillations in connectivity in the final state [Fig. 3.2(a1)].

Especially if the spatial distribution of cells is such that they do not all become equally strongly connected to their neighbours (as will happen with a random distribution), complex periodic behaviour can occur with individual cells displaying oscillations that differ in frequency and amplitude [see Fig. 3.2(b1)-(b4), (c1), (c2)]. The network as a whole will then show an overshoot with oscillations in connectivity (and electrical activity) in the final state, the amplitude of which will vary among different networks, depending on the distribution of ϵ values.

3.3.3 Simplifications

To derive a simplification, let us consider two cell types, X and Y, that differ only in their respective ϵ values, ϵ_X and ϵ_Y. As a spatial configuration that can occur in the network, we consider two X cells and two Y cells that, for simplicity, are placed in such a way that the X (Y) cells are identical to each other with respect to the overlap of their neuritic fields with those of the other cell type (Fig. 3.3), so that, starting with the same initial conditions, their dynamics will be the same: each X (Y) cell is, as it were, connected to itself. For the connection strengths between the cells, we have

$$\begin{aligned} W_{XX} &= \varphi(R_X)S \\ W_{YY} &= \varphi(R_Y)S \\ W_{XY} &= W_{YX} = \psi(R_X, R_Y)S = \xi(W_{XX}, W_{YY}), \end{aligned} \tag{3.9}$$

where W_{XX} (W_{YY}) is the connection strength between the two X (Y) cells with radius R_X (R_Y), W_{XY} is the connection strength between an X and Y cell, φ and ψ are functions determining the area of overlap between the cells [also see Eq. (3.3)], and $S > 0$ represents synaptic strength. For the dynamics of W (under the restriction that $W > 0$) we have

$$\begin{aligned} \frac{dW_{XX}}{dT} &= S\varphi'(R_X)\frac{dR_X}{dT} \\ \frac{dW_{YY}}{dT} &= S\varphi'(R_Y)\frac{dR_Y}{dT}. \end{aligned} \tag{3.10}$$

Since the outgrowing circular neuritic field is just one of the possible ways to model connectivity, we are not interested in the precise form of φ and

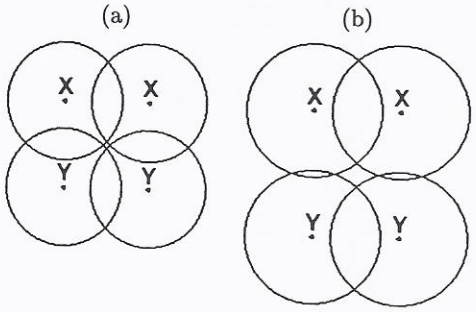

Fig. 3.3 The spatial distribution of the cells determines the relative connection strengths. **(a)** The connection strength between both X (Y) cells is the same as that between an X and Y cell. **(b)** The connection strength between both X (Y) cells is different from that between an X and Y cell.

ξ, which should not affect the essential findings. We therefore took simple functions φ and ξ, which indeed turned out to be sufficient for capturing the essential behaviour. We take φ such that $\varphi'(R) = a > 0$. Thus

$$\begin{aligned} \frac{dW_{XX}}{dT} &= Sa\frac{dR_X}{dT} = qG(X) \\ \frac{dW_{YY}}{dT} &= Sa\frac{dR_Y}{dT} = qG(Y), \end{aligned} \tag{3.11}$$

where $q = a\rho S$. The growth function G is taken to depend directly on the membrane potential instead of on the firing rate (this gives the same results, also in the network, see Van Ooyen & Van Pelt, 1994a), and, since the precise form of G is not crucial as long as it obeys Eq. (3.5), the simplest form of G is used: $G(X) = \epsilon_X - X$, $G(Y) = \epsilon_Y - Y$. For ξ we take

$$W_{XY} = p(W_{XX} + W_{YY}), \tag{3.12}$$

where p incorporates the spatial component (i.e., distance between the cells, see Fig. 3.3) that can cause the connection strength between the two X (Y) cells to be different from that between X and Y (if $p = 0.5$ and $W_{XX} = W_{YY}$, all connection strengths are the same).

Thus the complete model becomes

$$\begin{aligned}
\frac{dX}{dT} &= -X + (1-X)\,[W_{XX}F(X) + W_{XY}F(Y)] \\
\frac{dY}{dT} &= -Y + (1-Y)\,[W_{YY}F(Y) + W_{YX}F(X)] \\
\frac{dW_{XX}}{dT} &= q(\epsilon_X - X) \\
\frac{dW_{YY}}{dT} &= q(\epsilon_Y - Y) \\
W_{XY} &= W_{YX} = p(W_{XX} + W_{YY}).
\end{aligned} \tag{3.13}$$

In all the simulations, we use $q = 0.005$. An alternative interpretation of Eq 3.13 is that X and Y represent the average membrane potential of a population of X and Y cells, respectively (provided the variations among the individual cells are small relative to the average values, see Van Ooyen & Van Pelt, 1994a), and the W's the average connection strength impinging on a given cell.

The complex periodic behaviour seen in the network arises also in this simplified model. As already mentioned, the precise form of the functions φ, ψ (and ξ) is not essential. For example, if we take $\varphi(R_X) \sim R_X^2$, $\varphi(R_Y) \sim R_Y^2$ and $\psi(R_X, R_Y) \sim R_X R_Y$ [with $dR_X/dT = \rho G(X)$ and $dR_Y/dT = \rho G(Y)$] very similar results are obtained. In order to understand the basis for the occurrence of this behaviour, let us consider some further simplifications.

Model I

To study the effect of input on an X or Y cell, the following model is used:

$$\begin{aligned}
\frac{dX}{dT} &= -X + (1-X)\,[W_{XX}F(X) + I] \\
\frac{dW_{XX}}{dT} &= q(\epsilon_X - X).
\end{aligned} \tag{3.14}$$

There is only one cell type, and the input from Y in Eq. (3.13) is replaced by a constant input I. This enables us to show how the slow manifold of X, and consequently the behaviour of the system, changes under input. Increasing I causes the turning points of the manifold to move towards each other (in both W_{XX} and X) so that the hysteresis loop becomes smaller and finally disappears (Fig. 3.4).

For $\epsilon_X = 0.51$ and $I = 0$, for example, the system described by Eq. (3.14) shows oscillations (in W_{XX} and X) which become smaller for $I > 0$. They have disappeared when $I = 0.2$, under which condition the system shows

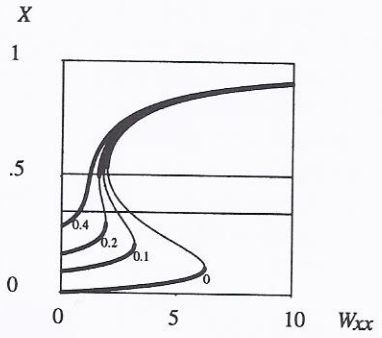

Fig. 3.4 External input makes the hysteresis loop of the slow manifold of X ($dX/dT = 0$) smaller [see Eq. (3.14)]. Shown are the manifolds for $I = 0$, 0.1, 0.2 and 0.4. The horizontal lines indicate the position of $\epsilon_X = 0.51$ and $\epsilon_X = 0.35$, respectively. The meaning of the bold lines is as in Fig. 3.1(a).

overshoot (starting with $W_{XX} = 0$). For $\epsilon_X = 0.35$ the system does not show overshoot no matter what the value of I. If ϵ_X is such that overshoot occurs for $I = 0$, it will also occur for higher values of I, until the hysteresis loop has disappeared.

Model II

Instead of a fixed input I, we now let the input to X be generated by Y. We further fix W_{XY} at a non-zero value, and set $W_{YX} = 0$ so that Y behaves independently of X. Thus

$$\begin{aligned}
\frac{dX}{dT} &= -X + (1 - X)\,[W_{XX}F(X) + W_{XY}F(Y)] \\
\frac{dY}{dT} &= -Y + (1 - Y)W_{YY}F(Y) \\
\frac{dW_{XX}}{dT} &= q(\epsilon_X - X) \qquad (3.15) \\
\frac{dW_{YY}}{dT} &= q(\epsilon_Y - Y) \\
W_{XY} &= C.
\end{aligned}$$

To describe the behaviour of this and subsequent models, we shall distinguish a number of different cases that are characterized by ϵ_X and ϵ_Y and the resulting behaviour in X and Y *when X and Y are uncoupled* (i.e., when

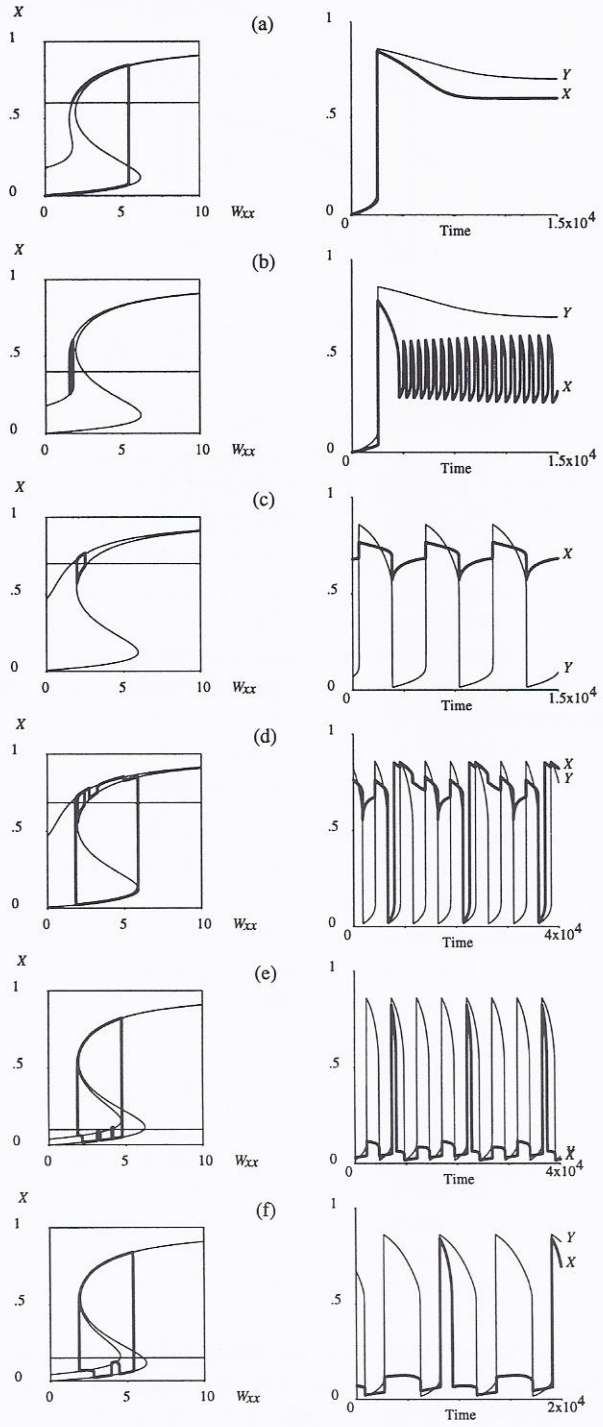
(a)
(b)
(c)
(d)
(e)
(f)
X
Y
Time
W_{XX}
1
.5
0
5
10
$1.5x10^4$
$4x10^4$
$2x10^4$

$W_{XY} = W_{YX} = 0$, which gives two independent equations identical to Eq. (3.14) with $I = 0$). Thus, ϵ_X (ϵ_Y) can be such that there is a stable point on the lower branch of the slow manifold of X (Y) [stable-lb], a stable point on the upper branch (stable-ub), or an unstable point, which causes regular oscillations. In Fig. 3.1(a) this corresponds to an intersection point on branch AB, CD or BC, respectively. The *coupling* between X and Y can give rise to complex periodic behaviour. In the following we give an inventory of the qualitatively different behaviours we found. In the figures, manifolds of X (Y) defined as $dX/dT = 0$ ($dY/dT = 0$) *for a given value of* Y (X), are drawn in the (W, X) [(W, Y)]-plane.

1. ϵ_Y = *stable-lb or stable-ub,* ϵ_X = *stable-lb or stable-ub.*

   Since there is no influence from X to Y, Y goes to ϵ_Y independently of ϵ_X, and $W_{XY}F(Y)$ becomes constant.

   That is, we end up with the same situation as in Eq. (3.14) with $I > 0$. The influence of Y does not change the stability of the points: X always goes to a stable point [Fig. 3.5(a)].

2. ϵ_Y = *stable-lb or stable-ub,* ϵ_X = *unstable.*

   Again $W_{XY}F(Y)$ becomes constant, and depending on the value of $W_{XY}F(\epsilon_Y)$

   - the oscillations in X (and W_{XX}) become smaller [Fig. 3.5(b)], or;
   - the oscillations disappear completely (i.e., stable point).

3. ϵ_Y = *unstable,* ϵ_X = *stable-ub or stable-lb.*

   In this case Y oscillates, and independently of X. Because of the nature of these oscillations (i.e., being the result of W_{YY} varying very slowly relative to the dynamics of Y), Y essentially jumps between values

---

Fig. 3.5 Behaviour of the model described by Eq. (3.15) for different values of ϵ_X and ϵ_Y. In each figure of the first column the bold line is the trajectory of the system in the (W_{XX}, X)-plane, the thin horizontal line indicates the value of ϵ_X, and the thin S-shaped lines are the manifolds of X defined as $dX/dT = 0$ for $Y = 0$ (lower curve) and $Y = 0.7$ (upper curve), respectively. In each corresponding figure of the second column, the behaviour of X (bold line) and Y is plotted against time. **(a)** $\epsilon_Y = 0.7$, $\epsilon_X = 0.6$, $W_{XY} = 0.25$. Note that the transition from quiescent to activated state takes place not at the turning point of the slow manifold but at a lower W_{XX} value because of the additional drive from Y. **(b)** $\epsilon_Y = 0.7$, $\epsilon_X = 0.4$, $W_{XY} = 0.25$. **(c)** $\epsilon_Y = 0.4$, $\epsilon_X = 0.7$, $W_{XY} = 1.0$. **(d)** $\epsilon_Y = 0.4$, $\epsilon_X = 0.685$, $W_{XY} = 1.0$. **(e)** $\epsilon_Y = 0.4$, $\epsilon_X = 0.1$, $W_{XY} = 0.045$. **(f)** $\epsilon_Y = 0.5$, $\epsilon_X = 0.15$, $W_{XY} = 0.05$. In all figures, except those of (a) and the time plot of (b), the initial transients are skipped.

on the lower branch (quiescent state) and values on the upper branch (activated state), while spending very little time at values in between. As is illustrated in Fig. 3.4, the manifold of X is different for a low or a high input (i.e., Y). In Fig. 3.5 the manifold of X is drawn for Y at the quiescent state (represented by $Y = 0$) and the activated state (represented by $Y = 0.7$). Since X attempts to follow its manifold, any time Y jumps from quiescent to activated state or vice versa, the behaviour of X can to a good approximation be described as jumping between these two manifolds (also see Fig. 3.6(a), in which the complete 3D picture is given).

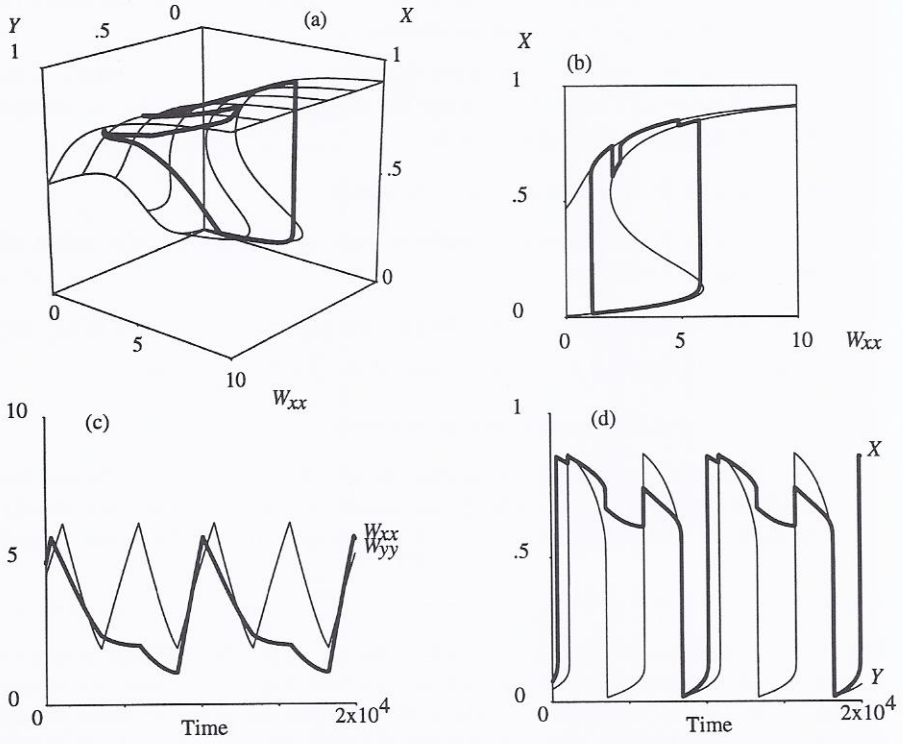

Fig. 3.6 Behaviour of the model described by Eq. (3.15) for $\epsilon_Y = 0.4$, $\epsilon_X = 0.6$, $W_{XY} = 1.0$. Initial transients are skipped. **(a)** The bold line is the trajectory of the system in (W_{XX}, X, Y)-space. The thin lines are the manifolds of X defined as $dX/dT = 0$ for different values of Y. **(b)** The bold line is the trajectory of the system in the (W_{XX}, X)-plane. The thin lines are the manifolds of X defined as $dX/dT = 0$ for $Y = 0$ (lower curve) and $Y = 0.7$ (upper curve), respectively. **(c)** W_{XX} (bold line) and W_{YY} against time. **(d)** X (bold line) and Y against time.

The oscillations in Y can cause X to make

- small oscillations (i.e., X stays at the upper branch if ϵ_X = stable-ub [Fig. 3.5(c)] or at the lower branch if ϵ_X = stable-lb);
- oscillations between quiescent and activated state, at the same frequency as those of Y;
- oscillations between quiescent and activated state, at a lower frequency than those of Y [Fig. 3.5(d), (e)].

4. ϵ_Y = *unstable,* ϵ_X = *unstable.*

X will oscillate between quiescent and activated state

- at the same frequency of Y;
- at a lower frequency of Y [Fig. 3.5(f)].

In all cases, ϵ_X and ϵ_Y determine not only whether or not oscillations occur when the cells are uncoupled, but also the relative speed with which X and Y move along their slow manifolds. Together with the strength of the interaction, W_{XY}, this determines the precise form of the oscillations when the cells are coupled. In Fig. 3.5(c), for example, Y drops to the quiescent state at a moment that X has reached a value such that X will not drop to the lower branch when Y is low. It does drop down when ϵ_X is only slightly smaller [as in Fig. 3.5(d)].

Model III

In the following model, X also influences Y, and the only difference from Eq. (3.13) is that $W_{XY} = W_{YX}$ is kept constant. Thus

$$\begin{aligned}
\frac{dX}{dT} &= -X + (1-X)\,[W_{XX}F(X) + W_{XY}F(Y)] \\
\frac{dY}{dT} &= -Y + (1-Y)\,[W_{YY}F(Y) + W_{YX}F(X)] \\
\frac{dW_{XX}}{dT} &= q(\epsilon_X - X) \\
\frac{dW_{YY}}{dT} &= q(\epsilon_Y - Y) \\
W_{XY} &= W_{YX} = C.
\end{aligned} \tag{3.16}$$

Note that, since the model is symmetrical in X and Y, the behaviour we find with ϵ_X = unstable and ϵ_Y is stable-ub, for example, is the same as with ϵ_Y = unstable and ϵ_X is stable-ub, interchanging X and Y.

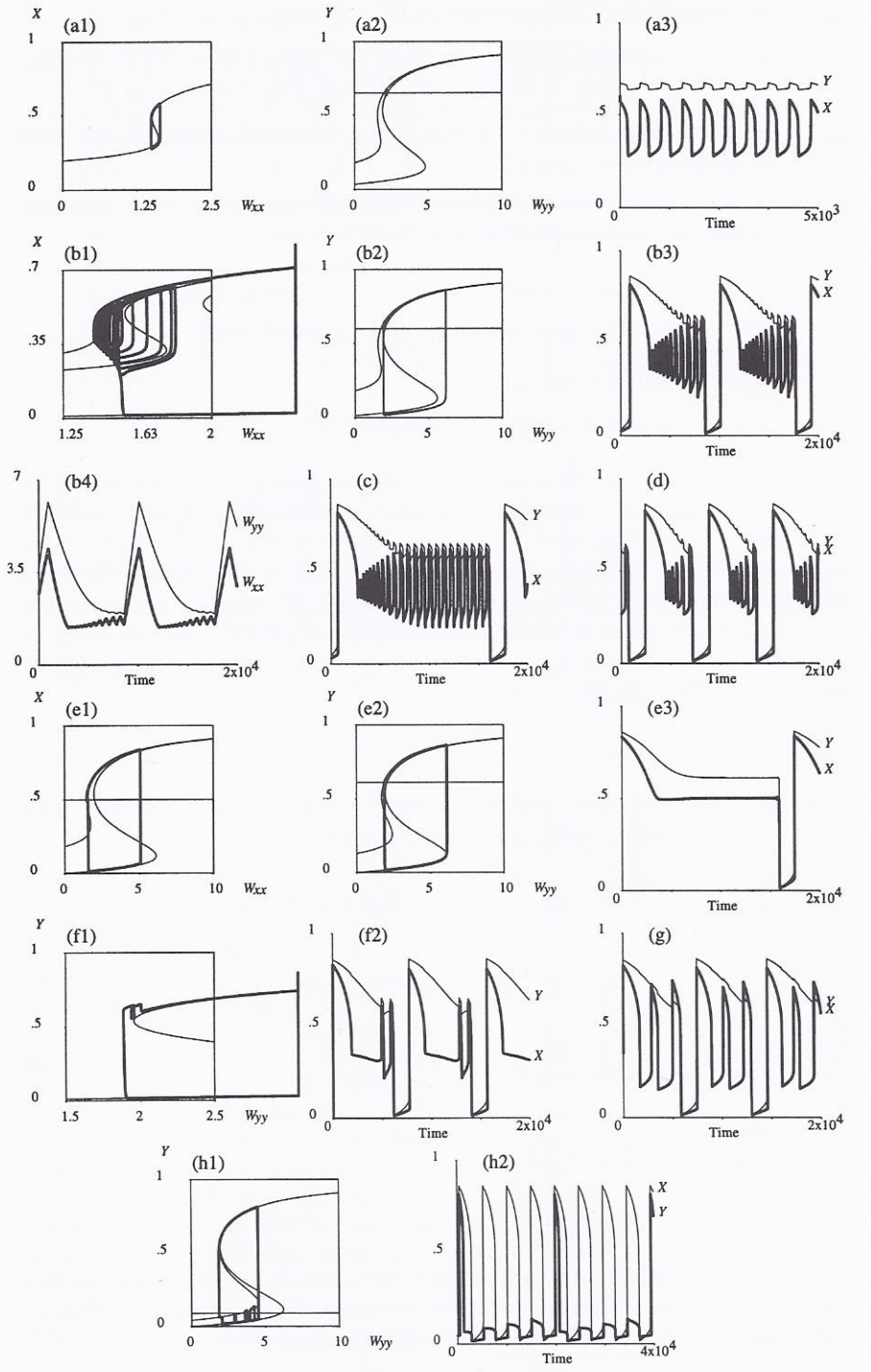
(a1)
(a2)
(a3)
(b1)
(b2)
(b3)
(b4)
(c)
(d)
(e1)
(e2)
(e3)
(f1)
(f2)
(g)
(h1)
(h2)
Time

1. ϵ_Y = *stable-lb or stable-ub,* ϵ_X = *stable-lb or stable-ub.*

   As in the previous models, the influence of X on Y and vice versa does not change the stability of the points: X and Y will always go to stable points. The interesting cases are those with one or both of the ϵ's unstable.

2. ϵ_X = *unstable,* ϵ_Y = *stable-ub.*

   - if W_{XY} is large enough Y can make X to go to a stable point;
   - with a smaller W_{XY}, X continues to oscillate while, since in contrast to the previous model X also influences Y, Y will oscillate as well, either remaining on the upper branch [Fig. 3.7(a1)-(a3)], or
   - if ϵ_Y is somewhat smaller, eventually falling down, together with X, to the lower branch [Fig 3.7(b1)-(b4)]. The periodicity of this pattern is determined by ϵ_Y: a slightly higher value results in a longer period [Fig. 3.7(c)], and a slightly smaller ϵ_Y results in a shorter period [Fig. 3.7(d)]. For some values, the period length is no longer constant: extremely long periods alternate 'chaotically' with much shorter ones (not shown);
   - if ϵ_X is such that only if Y is close to ϵ_Y, ϵ_X is in the oscillatory region, a type of behaviour as illustrated in Fig. 3.7(e1)-(e3) can be seen: Y moves slowly towards ϵ_Y and, when it is close enough, X suddenly drops down to the lower branch, as a result of which also Y falls. A lower value of ϵ_Y makes the process faster, resulting in a shorter period;

Fig. 3.7 Behaviour of the model described by Eq. (3.16) for different values of ϵ_X, ϵ_Y and W_{XY}. In each of the time plots the bold line indicates X [W_{XX} in (b4)] and the thin line Y [W_{YY} in (b4)], except in (h2). In each of the (W_{XX}, X) [(W_{YY}, Y)]-planes, the thin lines are the manifolds of X (Y) defined as $dX/dT = 0$ ($dY/dT = 0$) for a given value of Y (X); these values will be denoted below. The bold line in each plane is the trajectory of the system. In all figures the initial transients are skipped. **(a)** $\epsilon_Y = 0.65$, $\epsilon_X = 0.4$, $W_{XY} = 0.3$. **(a1)** $Y = 0.65$. **(a2)** $X = 0.3$ (lower curve) and $X = 0.6$ (upper curve). **(b)** $\epsilon_Y = 0.6$, $\epsilon_X = 0.4$, $W_{XY} = 0.3$. **(b1)** $Y = 0$ (lower curve), $Y = 0.6$ (middle curve), and $Y = 0.8$ (upper curve). **(b2)** $X = 0.2$ (lower curve), $X = 0.6$ (upper curve). **(c)** $\epsilon_Y = 0.604$, $\epsilon_X = 0.4$, $W_{XY} = 0.3$. **(d)** $\epsilon_Y = 0.56$, $\epsilon_X = 0.4$, $W_{XY} = 0.3$. **(e)** $\epsilon_Y = 0.61$, $\epsilon_X = 0.5$, $W_{XY} = 0.3$. **(e1)** $Y = 0$ (lower curve), $Y = 0.61$ (upper curve). **(e2)** $X = 0$ (lower curve), $X = 0.5$ (upper curve). **(f)** $\epsilon_Y = 0.58$, $\epsilon_X = 0.35$, $W_{XY} = 0.3$. **(f1)** $X = 0$. **(g)** $\epsilon_Y = 0.58$, $\epsilon_X = 0.35$, $W_{XY} = 0.15$. **(h)** $\epsilon_Y = 0.09$, $\epsilon_X = 0.4$, $W_{XY} = 0.05$. **(h1)** $X = 0$ (lower curve), $X = 0.7$ (upper curve). **(h2)** X and Y (bold line) against time.

- a kind of hybrid situation between Fig. 3.7(b3) and Fig. 3.7(e3) is seen in Fig. 3.7(f2). Because the relative speed with which X and Y move along their branches is now different, Y does initially not drop down to the low branch of its manifold but is just 'rescued' by the high branch, so that X can still make several oscillations. The relative speed with which X and Y move (which can be altered by changing ϵ_X and ϵ_Y) determines the number of these oscillations. W_{XY} determines the period of these oscillations: the lower W_{XY}, the larger the period [Fig. 3.7(g)].

3. ϵ_X = *unstable,* ϵ_Y = *stable-lb.*

   - for low ϵ_Y, Y makes small oscillations staying on the lower branch of its manifold, while X oscillates between quiescent and activated state;
   - if ϵ_Y is higher, Y can also make oscillations between quiescent and activated state, at the same frequency as those of X, or;
   - at a lower frequency [Fig. 3.7(h1), (h2)].

4. ϵ_X = *unstable,* ϵ_Y = *unstable.*

   As in the previous model, Y will oscillate between quiescent and activated state

   - at the same frequency of X;
   - at a lower frequency of X.

Full model

The last step to Eq. (3.13) is to have W_{XY} depend upon W_{XX} and W_{YY}, instead of being constant as in Eq. (3.16). With W_{XY} variable, we found the whole range of behaviours as described for Model III (with p ranging from 0.01 to 0.3). No qualitatively different behaviours could be found, possibly because the changes in W_{XY} are mostly, via W_{XX} and W_{YY}, parallel to those in X and Y, so that for the effective interactions [i.e., $W_{XY}F(Y)$ and $W_{XY}F(X)$] a constant value for W_{XY} does not affect the system very much.

Comparison with network model

A network consisting of a small group of cells of one type (characterized by its ϵ value) bordering to a much larger group of cells of another type, can, because of the large difference in cell number, be compared to simplified model II, in which cell Y (representing the largest population in the network) influences the other cell X, but not the other way around. In a network of this structure, the same patterns of periodic behaviour can be found as in the simplified model: compare, for example, Fig. 3.5(d) with Fig. 3.2(c1), (c2). Also the behaviour of simplified model III compares well with the patterns

found in the network: for example, compare Fig. 3.7(a3) with Fig. 3.2(a3), (a4), and Fig. 3.7(b3), (d) with Fig. 3.2(b1)-(b3). Thus, the interactions in the simplified models are sufficient to capture the essentials of the behaviours found in the network. Under point 2 of both simplified models II and III it is described that with a strong enough connection strength, the oscillations become smaller or disappear if the ϵ value of the other cell is in the stable region. This underlies the observation that when cells in a network become strongly connected to many of their neighbouring cells, the oscillations become smaller or disappear entirely if only a small proportion of the cells have an ϵ value in the stable region. Also the fact that complex periodic behaviour can occur especially when not all the cells become equally strongly connected to their neighbours, can be understood from the fact that a large interaction strength (a large W_{XY} in the simplified models) with a neighbouring cell that happens to have an ϵ value in the stable region would reduce the size of the oscillations or let them disappear.

3.3.4 Generalization

In the previous sections we have considered neurite outgrowth, which is an example of a slow activity-dependent process that attempts to stabilize neuronal activity by adapting an intrinsic cellular property. Another example of such a general process is postsynaptic receptor adaptation. After prolonged exposure to its own neurotransmitter, a receptor can become desensitized (e.g., Schwartz & Kandel, 1991). Also the number of receptors can be regulated, with down-regulation following an increase, and up-regulation following a decrease in electrical activity. For example in adult rat neocortex, an increase in neuronal activity or agonist stimulation decreases the number of AMPA receptors (a type of glutamate receptors) (Shaw and Lanius, 1992). Such control of receptor number and sensitivity may be regarded as a form of homeostasis of neuronal activity (Shaw & Lanius, 1992, also see Turrigiano *et al.*, 1994).

The following general model is used to study this process:

$$\begin{aligned}
\frac{dX}{dT} &= -X + (1-X)w_X\left[s_{XX}F(X) + s_{XY}F(Y)\right] \\
\frac{dY}{dT} &= -Y + (1-Y)w_Y\left[s_{YY}F(Y) + s_{YX}F(X)\right] \\
\frac{dw_X}{dT} &= g(\epsilon_X - X) \\
\frac{dw_Y}{dT} &= g(\epsilon_Y - Y).
\end{aligned} \tag{3.17}$$

In this model the number of connections or synapses (s_{XX}, s_{YY}, s_{XY} and s_{XY}) is fixed, whereas w_X (w_Y) is variable, e.g., representing the number

or effectiveness of the receptors of X (Y). In general, w_X (w_Y) represents any intrinsic (postsynaptic) cellular property that determines the effectiveness of all the cell's incoming connections. Thus, the variable that controls connection strength is not assigned to the interaction between two particular cells, but to the cell itself, so that, for a given cell, the strength of all its incoming connections is affected in the same way. The dynamics of w_X (w_Y) is such that neuronal activity is attempted to be maintained at a given level (ϵ_X and ϵ_Y, respectively). For simplicity we assume that $s_{XX} = s_{YY}$, and $s_{XY} = s_{YX}$, and transform Eq. (3.17) into

$$\begin{aligned} \frac{dX}{dT} &= -X + (1-X)W_X\,[F(X) + pF(Y)] \\ \frac{dY}{dT} &= -Y + (1-Y)W_Y\,[F(Y) + pF(X)] \\ \frac{dW_X}{dT} &= q(\epsilon_X - X) \\ \frac{dW_Y}{dT} &= q(\epsilon_Y - Y), \end{aligned} \tag{3.18}$$

where

$$\begin{aligned} W_X &= w_X s_{XX} \\ W_Y &= w_Y s_{YY} \\ p &= \frac{s_{XY}}{s_{XX}} = \frac{s_{YX}}{s_{YY}} \\ q &= g s_{XX} = g s_{YY}. \end{aligned} \tag{3.19}$$

Note, that compared with Eq. (3.13), W_{XY} and W_{YX} are missing. An interpretation of Eq. (3.18) in terms of neurite outgrowth would be that only the dendrites grow in an activity-dependent manner, while the axons do not react to electrical activity, and thus remain constant. In analogy to Eq. (3.13), X and Y can also be interpreted as representing the average membrane potential of a population of X and Y cells, respectively.

In order to study the effect of input onto a cell, we will consider, in analogy to Eq. (3.14), the following equation:

$$\frac{dX}{dT} = -X + (1-X)W_X\,[F(X) + I], \tag{3.20}$$

where $pF(Y)$ is replaced by a constant input I. As with Eq. (3.14), increasing I causes the turning points of the manifold of X to move towards each other, so that the hysteresis loop becomes smaller and finally disappears

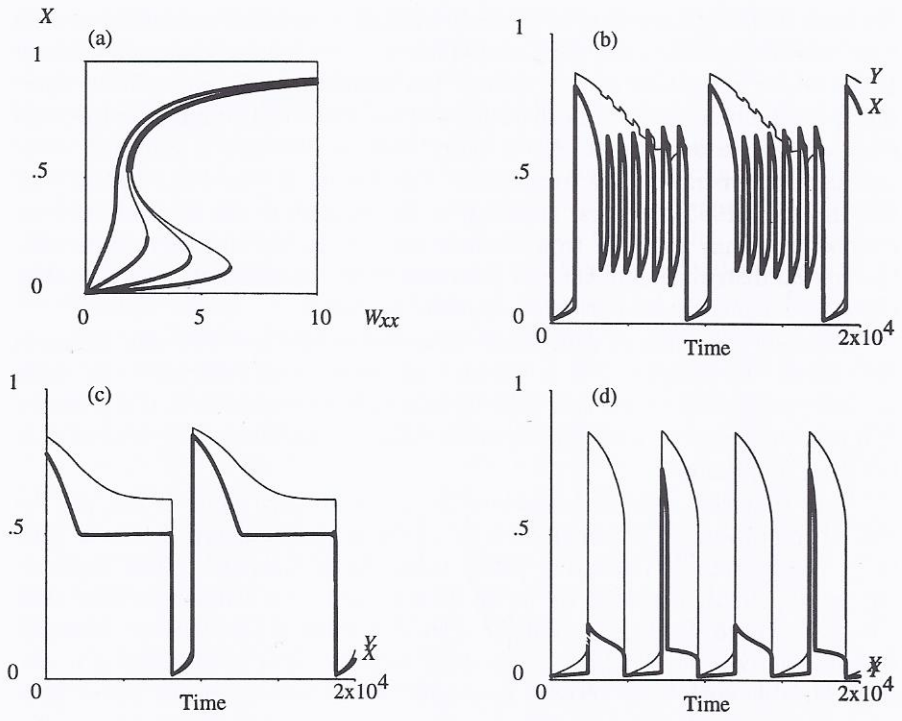

Fig. 3.8 **(a)** External input makes the hysteresis loop of the slow manifold of X ($dX/dT = 0$) smaller [see Eq. (3.20)]. Shown are the manifolds for $I = 0$, 0.01, 0.05 and 0.25. The meaning of the bold lines is as in Fig. 3.1(a). **(b)-(d)** Behaviour of the model described by Eq. (3.18). **(b)** $\epsilon_Y = 0.6$, $\epsilon_X = 0.4$, $p = 0.1$. X (bold line) and Y against time. **(c)** $\epsilon_Y = 0.62$, $\epsilon_X = 0.5$, $p = 0.18$. X (bold line) and Y against time. **(d)** $\epsilon_Y = 0.09$, $\epsilon_X = 0.4$, $p = 0.05$. Y (bold line) and X against time.

[Fig. 3.8(a)]. The only difference with Fig. 3.4 is that all the manifolds start in ($W_X = 0$, $X = 0$) because I has no effect when $W_X = 0$. Since the effect of I on the form of the manifolds is the same as with Eq. (3.14), the system described by Eq. (3.18) can be expected to show the entire range of behaviours as described for Model III and Eq. (3.13), as indeed it does [for examples see Fig. 3.8(b)-(d)]. The assumptions we made for s_{XX}, s_{YY}, s_{XY} and s_{YX} are not not crucial for these results.

3.4 Conclusions and Discussion

We have demonstrated that in a purely excitatory network composed of cells with differing neurite outgrowth properties (i.e., the level of electrical activity above which retraction occurs varies), the individual cells can exhibit complex periodic behaviour, in both outgrowth and electrical activity, on the time scale of neurite outgrowth. Even under these conditions, a transient overproduction of connectivity (overshoot: Van Ooyen & Van Pelt, 1994a; Van Ooyen *et al.*, 1995a) occurs, although in the final state the level of network connectivity may oscillate to a variable extent. In the full network model, the spatial distribution of the cell positions create connectivity patterns that allow for such complex periodic behaviour to occur.

Inclusion of inhibitory cells can be expected to lead to even richer dynamic properties. In Chapter 6 it is shown that, even if all cells have the same intrinsic outgrowth properties, activity-dependent outgrowth in the presence of inhibitory cells can lead, among other things, to an interesting type of slow bursting oscillations.

Note that the periodic behaviour described in this paper is not the result of inhibition, of external drive or of transmission delays between cells (e.g., Babloyantz & Destexhe, 1991; Destexhe & Gaspard, 1993; Houweling (*et al.*, 1995). Essential for its occurrence are: (i) a cellular variable that adapts slowly to electrical activity (electrical activity is here the fast variable) whereby activity levels above a specified 'setpoint' lead to alterations in the slow variable such that activity decreases, while activity levels below that setpoint lead to the slow variable being altered such that activity increases; (ii) different setpoints for different cells; (iii) a hysteresis relationship between electrical activity and the slow variable. This last condition can thus also be met in cases where hysteresis emerges as a property of only a large collection of cells (see e.g., Rose & Siebler, 1993). In our model hysteresis is already present in two inter-connected excitatory cells, and hinges upon (a) the firing rate function having a threshold for transition to a higher firing level and (b) low but non-zero values for sub-threshold membrane potentials. Conditions (a) and (b) are met by, for example, a sigmoidal firing rate function [the exact values of the parameters θ and α of the firing rate function are not crucial; also see Van Ooyen & Van Pelt (1994a) and Pakdaman *et al.*, (1994)].

For the above mentioned analysis and qualitative results to be valid, it is not necessary that the slow process be very much slower than the fast process: for example, with $q = 0.1$ (with a time constant of 1 for the neuronal dynamics), analysis in terms of slow manifolds is still warranted. The precise pattern, however, can be affected by q: a lower value than the one used, for example, results in more 'fast' oscillations within the pattern of Fig. 3.7(b3).

Provided that conditions (i), (ii) and (iii) are met, similar results will be obtained if the fast process (i.e., neuronal activity) is coupled, instead of to neurite outgrowth, to any other slow cellular process that acts to stabilize neuronal activity. For example, slow changes in ion channels that determine

the firing properties of a cell [in the model there is also a hysteresis relationship between electrical activity (X) and the firing threshold (θ)], or changes in neurotransmitter receptor sensitivity, as was examined in Section 3.3.4. A similar situation is described in Carpenter & Grossberg (1983), where a model of circadian rhythms is presented consisting of a four-dimensional fast-slow process in which the fast membrane potentials (described by shunting equations) interact with slowly accumulating chemical transmitter pools. The period of the rhythms is determined by the transmitter accumulation rate.

Since conditions (i), (ii) and (iii) for the generation of complex periodic behaviour are rather general, one might expect to see such oscillations in many different systems [for examples also see Murray (1989) and Rinzel & Ermentrout (1989)]. In tissue cultures of hippocampal neurons, for example, slow oscillations in neurite outgrowth have been observed (S. B. Kater, personal communication). Another example is the variability in firing rate on the order of several minutes, or even slower, which have been observed in tissue cultures of cerebral cortex cells (Ramakers *et al.*, 1990; Nuijtinck *et al.*, in preparation) as well as *in vivo* (e.g., Mirmiran & Corner, 1982). These fluctuations are usually associated with relatively long-lasting transients of network activity (so-called slow waves, recorded as field potentials) in the range of tens or hundreds of milliseconds, which alternate with periods of minimal activity (for references see Van Ooyen *et al.*, 1992b). Such patterns in which periods of increased network activity alternate with periods of minimal activity can - together with spontaneously firing cells to trigger network activity- be generated by slowly adapting processes, such as calcium-dependent potassium channels that act to hyperpolarize the cell after repeated firing (Van Ooyen *et al.*, 1992a).